

FQ-ViT: Fully Quantized Vision Transformer without Retraining

Yang Lin^{*†}, Tianyu Zhang^{*}, Peiqin Sun[‡], Zheng Li, Shuchang Zhou

MEGVII Technology

linyng.zhh@gmail.com, {zhangtianyu, sunpeiqin, lizheng02, zsc}@megvii.com

Abstract

Network quantization significantly reduces model inference complexity and has been widely used in real-world deployments. However, most existing quantization methods have been developed and tested mainly on Convolutional Neural Networks (CNN), and suffer severe degradation when applied to Transformer-based architectures. In this work, we present a systematic method to reduce the performance degradation and inference complexity of Quantized Transformers. In particular, we propose Powers-of-Two Scale (PTS) to deal with the serious inter-channel variation of LayerNorm inputs in a hardware-friendly way. In addition, we propose Log-Int-Softmax (LIS) that can sustain the extreme non-uniform distribution of the attention maps while simplifying inference by using 4-bit quantization and the BitShift operator. Comprehensive experiments on various Transformer-based architectures and benchmarks show that our methods outperform previous works in performance while using even lower bit-width in attention maps. For instance, we reach 85.17% Top-1 accuracy with ViT-L on ImageNet and 51.4 mAP with Cascade Mask R-CNN (Swin-S) on COCO. To our knowledge, we are the first to achieve comparable accuracy degradation ($\sim 1\%$) on fully quantized Vision Transformers. Code is available at <https://github.com/linyng-zhh/FQ-ViT>.

1 Introduction

Transformer-based architectures have achieved competitive performance in various computer vision (CV) tasks, including image classification [9, 39, 31], object detection [4, 31], semantic segmentation [46] and so on. Compared to the CNN counterparts, Transformers usually have more parameters and higher computational costs. For example, ViT-L [9] has 307M parameters and 190.7G FLOPs, reaching the accuracy of 87.76% in ImageNet with large-scale pre-training. However, the large number of parameters and computational overhead of Transformer-based architectures present a challenge when deployed to resource-constrained hardware devices.

To facilitate deployment, several techniques have been proposed, including quantization [47, 10, 33, 36, 25], pruning [15, 13], distillation [19, 35] and adaptation of architecture design [20, 38, 12]. We focus on the quantization

^{*}Equal contribution.

[†]Work done while interning at MEGVII Technology.

[‡]Corresponding author.

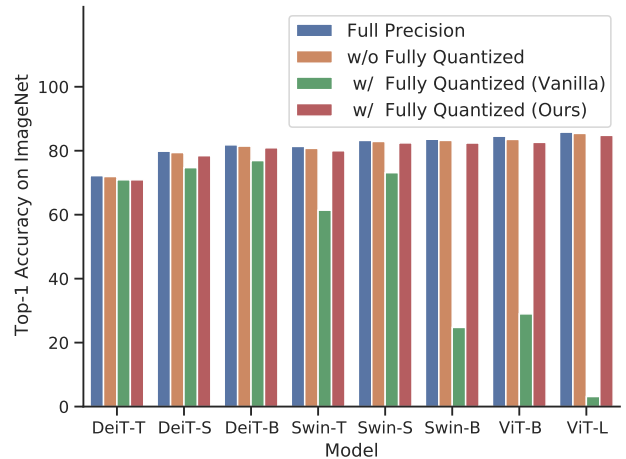


Figure 1: Top-1 accuracy on ImageNet for full precision and quantized Vision Transformers. w/o Fully Quantized: LayerNorm and Softmax remain floating-point, other modules quantized to 8-bit with MinMax. w/ Fully Quantized (Vanilla): all modules quantized to 8-bit with MinMax. w/ Fully Quantized (Ours): apply PTS and LIS to Vanilla.

technique in this paper and note that pruning, distillation, and architecture adaptation are orthogonal to our work and hence can be combined.

Most existing quantization approaches have been designed and tested on CNNs and lack proper handling of Transformer-specific constructs. Previous work [32] found there would be significant accuracy degradation when quantizing LayerNorm and Softmax of Transformer-based architectures. So we revisit these two exclusive modules of the Vision Transformers and discover the reasons for degradation. Firstly, we find a serious inter-channel variation of LayerNorm inputs, which some channel ranges even exceed 40x of the median. Traditional methods cannot handle such large fluctuations of activations, which leads to large quantization errors. Many approaches propose to use channel-wise quantization, but would introduce additional hardware design and inference overhead. Secondly, we find that the values of the attention map have an extreme non-uniform distribution, with most values clustered in $0 \sim 0.01$, and fewer

high attention values close to 1 existing. While it is acceptable in 8-bit quantization, most attention values will be deactivated when reduced to 4-bit.

Based on the analysis above, we propose Powers-of-Two Scale (PTS) to quantize the inputs of the LayerNorm. In this way, BitShift operation is adopted to quantize different channels individually with only one layer-wise quantization scale. In addition, we propose Log-Int-Softmax (LIS), which provides higher quantization resolution for small values and presents a more efficient integer inference for Softmax. To our best knowledge, we are the first to propose a fully quantized Vision Transformer without retraining. As shown in Figure 1, our method significantly improves the performance of fully quantized Vision Transformers and achieves comparable accuracy with full precision counterpart.

Our contributions are three-fold:

- Powers-of-Two Scale (PTS) significantly reduces the extreme inter-channel variations present in inputs of LayerNorm, and strikes a balance between high efficiency of layer-wise quantization and high precision of channel-wise quantization;
- Log-Int-Softmax (LIS) performs 4-bit quantization for attention maps, replacing multiplication with BitShift and giving an integer-only inference for Softmax, which significantly improves efficiency with little accuracy drop;
- We conduct extensive experiments on image classification and object detection with various Transformer-based architectures. The results show that our fully quantized Vision Transformers with 8-bit weights/activations and 4-bit attention maps, can achieve performance comparable to floating-point versions.

2 Related Work

2.1 Vision Transformer

Recently, Transformer-based architectures show great power in CV tasks. ViT [9] pioneered applying a pure Transformer [40] directly to sequences of image patches and showed great performance. Emerging works based on ViT demonstrated the effectiveness of Vision Transformers across high-level tasks such as classification [39, 14, 43, 41], detection [4, 6, 48] and segmentation [46, 37], as well as low-level tasks [42, 5]. The newly proposed Swin Transformer [31] even surpassed the state-of-the-art CNNs on most CV tasks, presenting strong expressive and generalization capability of Transformer. However, these high-performing Vision Transformers are attributed to the large number of parameters and high computational overhead, limiting their adoption. Therefore, innovating a smaller and faster Vision Transformer becomes a new trend. LV-ViT [24] is equipped with a token labeling method. CCT [16] is constructed with convolutions and a sequence pooling strategy. These two works both significantly reduced the number of parameters. Le-ViT [12] made progress in faster inference with down-sampling, patch descriptors, and a redesign of Attention-MLP block. DynamicViT [34] presented a dynamic token sparsification framework to prune redundant to-

kens progressively and dynamically, achieving very competitive complexity/accuracy trade-offs. Evo-ViT [44] proposed a slow-fast updating mechanism that guarantees information flow and spatial structure, trimming down both the training and inference complexity. While the above works focus on efficient model designing, this paper boosts the compression and acceleration in the track of quantization.

2.2 Network Quantization

Current quantization methods can be divided into two categories: Quantization-Aware Training (QAT) and Post-Training Quantization (PTQ). QAT [47, 23, 11, 7, 10] depends on training to achieve aggressively low-bit (e.g. 2-bit) quantization and promising performance, while it often requires a high-level expert knowledge and huge GPU resources for training or fine-tuning. To reduce above costs of quantization, PTQ, which is training-free, has received more widespread attention and lots of excellent works arise. OMSE [8] proposed to determine the value range of activation by minimizing the quantization error. AdaRound [33] presented a novel rounding mechanism to adapt the data and the task loss. AdaQuant [21] expanded the optimization space based on AdaRound and utilized a sequential method to improve the performance of quantized models. BRECQ [28] analyzed the second-order error based on the Gauss-Newton matrix and proposed block reconstruction to achieve a good balance between cross-layer dependency and generalization error. Besides works above specific to CNNs, [32] proposed a post-training quantization method for Vision Transformers with similarity-aware and rank-aware strategies. However, this work did not quantize Softmax and LayerNorm, resulting in an incomplete quantization.

3 Proposed Method

3.1 Preliminary

In this section, we explain the notations of network quantization. Assuming the quantization bit-width is b , the quantizer $Q(\cdot)$ can be formulated as a function that maps a floating-point number $X \in \mathbb{R}$ to the nearest quantization bin:

$$Q(\cdot|b) : \mathbb{R} \rightarrow q, \quad (1)$$

$$q = \begin{cases} \{-2^{b-1}, \dots, 2^{b-1} - 1\} & \text{Signed,} \\ \{0, 1, \dots, 2^b - 1\} & \text{Unsigned.} \end{cases} \quad (2)$$

There are various quantizer $Q(\cdot)$, where uniform [23] and Log2 [2] are typically used.

Uniform Quantization is well supported on most hardware platforms. Its quantizer $Q(\cdot|b)$ can be defined as:

$$Q(X|b) = \text{clip}(\lfloor \frac{X}{S} \rfloor + Z, 0, 2^b - 1), \quad (3)$$

where S (scale) and Z (zero-point) are quantization parameters determined by the lower bound l and the upper bound

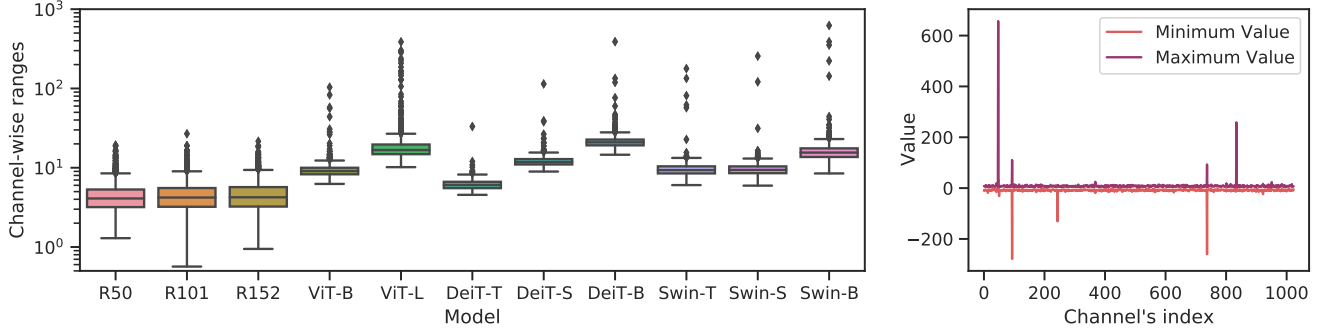


Figure 2: **Left:** Boxplot of the last LayerNorm inputs’ channel-wise ranges in each model. **Right:** Channel-wise minimum and maximum values of the last LayerNorm inputs in full precision Swin-B. The above two figures show that there exists more serious inter-channel variation in Vision Transformers than CNNs, which leads to unacceptable quantization errors with layer-wise quantization.

u of X , which are usually minimum and maximum values:

$$l = \min(X), u = \max(X), \quad (4)$$

$$S = \frac{u - l}{2^b - 1}, \quad (5)$$

$$Z = \text{clip}(\lfloor -\frac{l}{S} \rfloor, 0, 2^b - 1). \quad (6)$$

Log2 Quantization converts the quantization process from linear to exponential variation. Its quantizer $Q(\cdot|b)$ can be defined as:

$$Q(X|b) = \text{sign}(X) \cdot \text{clip}(\lfloor -\log_2 \frac{|X|}{\max(|X|)} \rfloor, 0, 2^{b-1} - 1). \quad (7)$$

In this paper, all modules are quantized, including Conv, Linear, LayerNorm, Softmax, etc. To meet the existing hardware platforms as much as possible, we apply uniform quantization for weights and activations. Especially for attention maps, we perform aggressively low-bit Log2 quantization and give an integer-only inference solution based on BitShift rather than multiplication.

3.2 Powers-of-Two Scale for LayerNorm Quantization

During inference, LayerNorm [1] computes the statistics μ_X, σ_X in each forward step and normalizes input X . Then, affine parameters γ, β rescale the normalized input to another learned distribution. The above process can be written as:

$$y = \frac{X - \mu_X}{\sqrt{\sigma_X^2 + \epsilon}} \cdot \gamma + \beta. \quad (8)$$

Unlike BatchNorm [22], commonly used in CNNs, LayerNorm cannot be folded into the previous layer due to its dynamic computational property, so we have to quantize it separately. However, significant performance degradation will be exposed while applying post-training quantization on it. Looking into the inputs of LayerNorm layers, we find serious inter-channel variation. Figure 2 presents the channel-wise ranges of activations in the last LayerNorm layer. In

addition, we also display the cases of ResNets [18] for comparison. Considering that there is no LayerNorm in ResNets, we choose the activations at the same position (fourth stage’s outputs) to exhibit.

It is observed that the channel-wise ranges fluctuate more wildly in Vision Transformers than those in ResNets. For instance, the maximum range/median range of ResNet152 is only 21.6/4.2, while it goes up to 622.5/15.5 in Swin-B. Based on such extreme inter-channel variation, layer-wise quantization, which applies the same quantization parameters to all channels, will lead to an intolerable quantization error. A possible solution is channel-wise quantization, which assigns different quantization parameters to each channel. However, this will induce the calculation of mean and variance in the floating-point domain, causing a high hardware overhead.

Taking the advantages of both layer-wise and channel-wise quantization, we propose Powers-of-Two Scale (PTS) for LayerNorm’s quantization. The core idea of PTS is to equip different channels with different Powers-of-Two Scale factors, rather than different quantization parameters. Given the quantization bit-width b , the input activation $X \in \mathbb{R}^{B \times L \times C}$, the layer-wise quantization parameters $S, Z \in \mathbb{R}^1$, and the Powers-of-Two Scale factors $P = [p_1, p_2, \dots, p_C] \in \mathbb{N}^C$, then the quantized activation X_Q can be formulated as:

$$X_Q = Q(X|b) = \text{clip}(\lfloor \frac{X}{2^{P_c} S} \rfloor + Z, 0, 2^b - 1), \quad (9)$$

with

$$S = \frac{\max(X) - \min(X)}{2^b - 1} / 2^K, \quad (10)$$

$$Z = \text{clip}(\lfloor -\frac{\min(X)}{S} \rfloor, 0, 2^b - 1), \quad (11)$$

$$p_c = \arg \min_{p_c \in \{0, 1, \dots, K\}} \|X_c - \lfloor \frac{X_c}{2^{p_c} S} \rfloor \cdot 2^{p_c} S\|^2. \quad (12)$$

Noticing c represents the channel index for X and P . The hyper-parameter K could meet different scaling requirements. In order to cover the different inter-channel variants

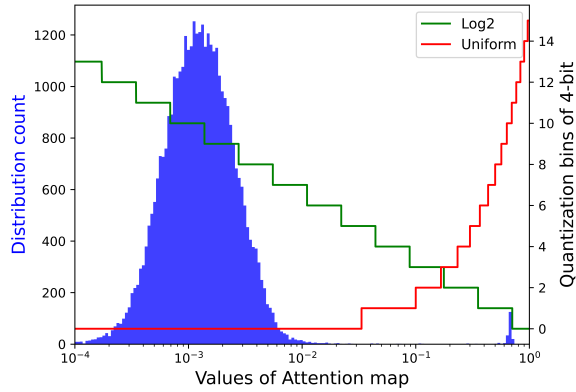


Figure 3: Distribution of the attention map values from the first layer of ViT-L, and visualizing the quantized bins using uniform or Log2 quantization with 4-bit. Log2 preserves more quantization bins than uniform for the small value interval with dense distribution.

across all models, we set $K = 3$ as default. Detailed experiments can be found in Section 4.4.

At this point, each channel has its own PTS factors P and layer-wise parameters S, Z . During inference, layer-wise parameters S and Z can be extracted so the computation of μ, σ could be done in the integer domain rather than floating-point, which reduces the energy and area costs [29]. Meanwhile, thanks to the nature of powers-of-two, PTS factors P can be efficiently combined with layer-wise quantization by BitShift operator. The whole process can be processed with two phases:

Phase 1: Shift the quantized activation with PTS factors:

$$\widehat{X}_Q = (X_Q - Z) \lll P. \quad (13)$$

Phase 2: Calculate the mean and variance based on the shifted activation \widehat{X}_Q :

$$\mu(X) \approx \mu(2^P S \cdot (X_Q - Z)) = S \cdot \mu(\widehat{X}_Q), \quad (14)$$

$$\sigma(X) \approx \sigma(2^P S \cdot (X_Q - Z)) = S \cdot \sigma(\widehat{X}_Q). \quad (15)$$

3.3 Log-Int-Softmax for Softmax Quantization

Multi-Head Self-Attention (MSA) is one of the most important components in Transformer-based architectures, while it is considered the most resource-intensive due to the quadratic complexity to the number of token, the division of the image resolution by the patch size. As model performance proved to benefit from higher resolution [38] and smaller patch size [9], when the increasing resolution and reducing patch size, the storage and computation of attention map become the bottleneck which directly affect the throughput and latency of inference. Therefore, smaller attention maps and more efficient inference become an urgent need.

Log2 Quantization for Attention Map In order to compress the attention map to smaller size and speed up the inference, we quantize the attention map to lower bit-width.

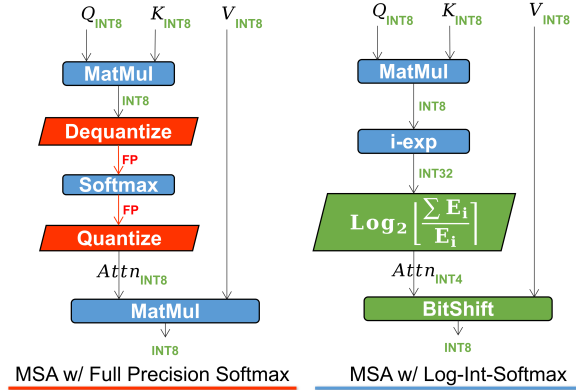


Figure 4: Comparison of using full precision Softmax and Log-Int-Softmax in quantized multi-head self-attention inference. Full precision Softmax needs to dequantize and re-quantize around Softmax. LIS keeps an integer-only stream in the whole MSA inference.

As we experimenting on quantizing the attention map from 8-bit to 4-bit with uniform quantization, all Vision Transformers show severe performance drop. For example, DeiT-T only results in 8.69% Top-1 accuracy on ImageNet with 4-bit uniform quantized attention maps, decreasing 63.05% from 8-bit case.

Inspired by the idea of sparse attention in Vision Transformers [34], we probe into the distribution of attention maps, as Figure 3 shows. We observe a distribution centering at a fairly small value, while only few outliers have larger values close to 1. Averaging on all attention maps in ViT-L, about 98.8% of values in attention map are smaller than $1/16$. Comparing with 4-bit uniform quantization only assigns 1 bin, Log2 method allocates 12 bins for 98.8% of the values. Moreover, following the purpose of ranking-aware loss [32], Log2 quantization can retain the order consistency between full precision and quantized attention maps. As a result, we save the extreme degradation in 4-bit quantization of attention map and achieve equal performance as 8-bit uniform quantization with 50% less computational consumption.

Log2 quantization proved to be suitable combining with Softmax from two aspects. Firstly, comparing to Equation 7, the fixed output range $(0, 1)$ of Softmax makes the Log2 function calibration-free:

$$\text{Attn}_Q = Q(\text{Attn} | b) = \text{clip}(\lfloor -\log_2(\text{Attn}) \rfloor, 0, 2^b - 1). \quad (16)$$

Secondly, it also introduces the merits of converting the Multiply operator to BitShift in the multiplication between the quantized attention map Attn_Q and values V_Q as:

$$\text{Attn} \cdot V_Q = V_Q \lll (N - \text{Attn}_Q). \quad (17)$$

Noticing that directly right shift V_Q with the results of Log2 may lead to severe truncation errors. We use $N - \text{Attn}_Q$ as the quantized output with a scale equaling $1/2^N$, which ensures a left-shift operation to prevent from truncation loss. With the substitution of multiplication with BitShift operation, we can retain less latency and larger throughput.

Method	W/A/Attn Bits	ViT-B	ViT-L	DeiT-T	DeiT-S	DeiT-B	Swin-T	Swin-S	Swin-B
Full Precision	32/32/32	84.53	85.81	72.21	79.85	81.85	81.35	83.20	83.60
PTQ for ViT [32]	8/8/8	-	-	-	77.47	80.48	-	-	-
MinMax	8/8/8	23.64	3.37	70.94	75.05	78.02	64.38	74.37	25.58
MinMax w/ PTS	8/8/8	83.31	85.03	71.61	<u>79.17</u>	81.20	80.51	82.71	82.97
MinMax w/ PTS, LIS	8/8/4	82.68	84.89	71.07	78.40	80.85	80.04	82.47	82.38
EMA [23]	8/8/8	30.30	3.53	71.17	75.71	78.82	70.81	75.05	28.00
EMA w/ PTS	8/8/8	<u>83.49</u>	85.10	71.66	79.09	<u>81.43</u>	80.52	82.81	83.01
EMA w/ PTS, LIS	8/8/4	82.57	85.08	70.91	78.53	80.90	80.02	82.56	82.43
Percentile [27]	8/8/8	46.69	5.85	71.47	76.57	78.37	78.78	78.12	40.93
Percentile w/ PTS	8/8/8	80.86	85.24	<u>71.74</u>	78.99	80.30	<u>80.80</u>	82.85	<u>83.10</u>
Percentile w/ PTS, LIS	8/8/4	80.22	85.17	71.23	78.30	80.02	80.46	82.67	82.79
OMSE [8]	8/8/8	73.39	11.32	71.30	75.03	79.57	79.30	78.96	48.55
OMSE w/ PTS	8/8/8	82.73	<u>85.27</u>	71.64	78.96	81.25	80.64	<u>82.87</u>	83.07
OMSE w/ PTS, LIS	8/8/4	82.37	85.16	70.87	78.42	80.90	80.41	82.57	82.45

Table 1: Comparison with post-training quantization baselines in Top-1 accuracy on ImageNet benchmark. The numbers in Underline represent the best performance with PTS and the numbers in **Bold** represent the best performance with PTS and LIS.

Integer-only Inference Previous works [32, 45] chose not to quantize Softmax because the negligibility of the parameter amount in Softmax, and quantization may lead to significant accuracy degradation. However, data moving between CPU and GPU/NPU, doing dequantization and requantization, will induce great difficulties in hardware design, which is not a negligible consumption.

Combining Log2 quantization with i-exp, which is a polynomial approximation of exponential function presented by [25], we propose Log-Int-Softmax, an integer-only, faster, low consuming Softmax:

$$\exp(S \cdot X_Q) \approx S' \cdot \text{i-exp}(X_Q), \quad (18)$$

$$\text{LIS}(S \cdot X_Q) = N - \log_2 \left\lceil \frac{\sum \text{i-exp}(X_Q)}{\text{i-exp}(X_Q)} \right\rceil, \quad (19)$$

with $N = 2^b - 1$. An integer Log2 function can be easily implemented by using BitShift to find the Most Significant Bit (MSB), and adding the value of bit right behind it. Detailed derivation can be found in the supplementary materials.

The two parts above are integrated as Figure 4 shows, with the data type of every stage labeled. In the multi-head self-attention with unquantized Softmax shown on the left, the matrix multiplication of Q and K needs to be dequantized to full precision before Softmax, and requantized after it. When Log-Int-Softmax adopted, shown on the right, the entire data stream can be in pure integer, with quantization scale individually and paralleling calculated. In conclusion, we propose an integrated quantization solution named Log-Int-Softmax, performing an integer-only data stream, quantizing the attention map to 4-bit, and using BitShift instead of Multiply, which greatly improves the efficiency and reduces the overhead.

4 Experiments

In this section, we present experimental results on Vision Transformers for image classification and object detection. We state the detailed experimental configuration firstly and

then exhibit the comparison of the proposed method with existing post-training quantization baselines in ImageNet [26] and COCO [30] benchmarks. In the end, ablation studies are conducted to evaluate the effectiveness of Powers-of-Two Scale (PTS) and Log-Int-Softmax (LIS).

4.1 Implementation Details

Experimental Settings We randomly sample 1000 training images from ImageNet or COCO as the calibration data, and use the validation set to evaluate performance. Apart from special notes, we perform symmetric channel-wise quantization for weights and asymmetric layer-wise quantization for activations. For a fair comparison, the quantization method for weights is fixed as MinMax. The hyperparameter K in Powers-of-Two Scale is set to 3.

Comparison Methods This paper employs several current post-training quantization strategies, including MinMax, EMA [23], Percentile [27], OMSE [8] and PTQ for ViT [32]. MinMax uses the minimum and maximum values of the total data as the clipping values; EMA [23] is based on MinMax and uses an average moving mechanism to smooth the minimum and maximum values of different mini-batch; Percentile [27] assumes that the distribution of values conforms to a normal distribution and uses the percentile to clip. In this paper, we use the 1e-5 percentile because the 1e-4 commonly used in CNNs has poor performance in Vision Transformers. OMSE [8] determines the clipping values by minimizing the quantization error. PTQ for ViT [32] proposed similarity-aware and ranking-aware methods to obtain the best quantization parameters and was the state-of-the-art post-training quantization method for Vision Transformers to the best of our knowledge. However, PTQ does not quantize the LayerNorm and Softmax, while we quantize all modules.

It is worth noting that our methods are orthogonal to others, so we apply the proposed PTS and LIS to these baselines in the following experiments.

Method	W/A/Attn Bits	Mask R-CNN w/ Swin-S	Cascade Mask R-CNN w/ Swin-S
Full Precision	32/32/32	48.5	52.0
MinMax	8/8/8	32.8	35.2
MinMax w/ PTS	8/8/8	47.8	51.4
MinMax w/ PTS, LIS	8/8/4	47.2	50.8
EMA [23]	8/8/8	37.9	40.4
EMA w/ PTS	8/8/8	48.1	51.5
EMA w/ PTS, LIS	8/8/4	47.7	51.3
Percentile [27]	8/8/8	41.6	44.7
Percentile w/ PTS	8/8/8	48.1	51.6
Percentile w/ PTS, LIS	8/8/4	47.7	51.4
OMSE [8]	8/8/8	42.6	44.9
OMSE w/ PTS	8/8/8	<u>48.2</u>	<u>51.7</u>
OMSE w/ PTS, LIS	8/8/4	47.7	51.2

Table 2: Comparison with post-training quantization baselines in bbox mAP on COCO benchmark. The numbers in Underline represent the best performance with PTS and the numbers in **Bold** represent the best performance with PTS and LIS.

4.2 Image Classification on ImageNet

To demonstrate the effectiveness of proposed methods, We conduct extensive experiments in ImageNet [26] with various Vision Transformers, i.e., ViT [9], DeiT [39], Swin Transformer [31]. Specifically, for the DeiT and Swin Transformer series, we use the models trained on ImageNet-1k, while for the ViT series, we use the models pre-trained on ImageNet-22k and fine-tuned on ImageNet-1k. The overall results are reported in Table 1.

In each row of the Table 1, we compare the quantization Top-1 accuracy of the baselines and the variant methods combining PTS and LIS on each model. We can see that all traditional methods have a significant accuracy drop on Transformer-based models. For instance, MinMax suffers a 60.89% accuracy drop on ViT-B, and the clipping-based method OMSE [8] suffers a 11.14% drop, comparing to the full precision model. The proposed PTS significantly improves the quantization accuracy for all existing baselines and achieves a nearly lossless 8-bit post-training quantization. Also, the results show that proposed LIS achieves 4-bit quantization for attention maps and integer-only attention inference with $\sim 0.5\%$ accuracy drop on each model. In conclusion, we achieve new state-of-the-art results on the post-training quantization for Vision Transformers with average 1% accuracy degradation.

4.3 Object Detection on COCO

We also conduct experiments on the object detection benchmark COCO [30]. We choose Swin series [31] detectors for experiments and the results can be found in Table 2. It is observed that all baselines have poor performance on fully quantized detectors. For example, MinMax loses 15.7 mAP in Mask R-CNN [17] (Swin-S) and 16.8 mAP in Cascade Mask R-CNN [3, 17] (Swin-S), while OMSE [8] achieves the best results among baselines, but there is still a loss of >5.0 mAP. By combining our methods proposed in this paper, the performance of all detectors significantly increase, achieving 47.7 mAP on Mask R-CNN (Swin-S) and 51.3

Model	FP	Non-Quantized	Quantized	PTS
ViT-B	84.53	83.46	23.64	83.23
ViT-L	85.81	85.37	3.37	85.11
DeiT-T	72.21	71.74	70.94	71.77
DeiT-S	79.85	79.42	75.05	79.27
DeiT-B	81.85	81.48	78.02	81.32
Swin-T	81.35	80.70	64.38	80.38
Swin-S	83.20	82.94	74.37	82.73
Swin-B	83.60	83.26	25.58	82.96

Table 3: Comparison between different quantization strategies for LayerNorm. Non-Quantized means all LayerNorm layers are in floating-point type and Quantized means all LayerNorm layers are quantized by MinMax.

mAP on Cascade Mask R-CNN (Swin-S) with 8-bit on weights/activations and 4-bit on attention maps.

4.4 Ablation Studies

Effect of Powers-of-Two Scale (PTS) To evaluate the effectiveness of Powers-of-Two Scale (PTS), we compare different quantization strategies for LayerNorm layers, including non-quantized, layer-wise MinMax quantized and PTS. We implement these three methods for inputs of all LayerNorm layers and the other layers are quantized by MinMax.

The detailed results are shown in Table 3. We observe that there is only a little accuracy degradation for the models with non-quantized LayerNorm, while they suffer a significant drop when applying quantization. For instance, accuracy for ViT-L drops from 85.37% to 3.37% after quantizing LayerNorm. However, with proposed PTS, all models achieve a high accuracy improvement and the final results approach that of non-quantized LayerNorm.

In addition, as shown in Figure 5, we conduct experiments on the effect of hyper-parameter K in PTS. We find that all models' performance are saturated when $K = 3$. Therefore, we take the default value as 3 to obtain better performance

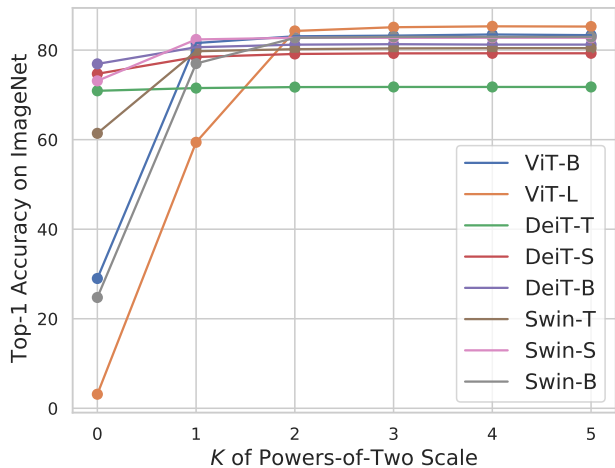


Figure 5: Top-1 accuracy on ImageNet with different hyperparameter K.

on all models.

Effect of Log-Int-Softmax (LIS) In this section, we evaluate the effect of the proposed Log2 quantization and integer inference wrapping in LIS when using different bit-width. The experimental results are shown in Table 4, while LayerNorm using full precision, and MinMax is chosen for the uniform quantization as a baseline. As we can see, Log2 quantization is able to rescue the 4-bit case from huge accuracy drop brought by uniform quantization. In addition, the proposed integer inference performs robustly as the last column of the table shows, only inducing less than 0.5% accuracy drop.

We visualize the attention map to see the difference between uniform and Log2 quantization as Figure 6 shows. When both using 8-bit, uniform quantization focuses on the high activation area, while Log2 keeps more texture in the low activation area, which retains more relative rank of the attention map. This divergence does not make a big difference in the case of 8-bit. However, when quantized to lower bit-width, as the 6-bit and 4-bit cases show, uniform quantization sharply degrades and even deactivates all the attention area. On the contrary, Log2 quantization still presents acceptable performance similar to 8-bit.

5 Conclusions

In this paper, we propose a method to fully quantize Vision Transformers. Specifically, we propose Powers-of-Two Scale (PTS) to deal with the serious inter-channel variations in the inputs of LayerNorm. In addition, we propose an integrated quantization solution Log-Int-Softmax (LIS) to implement 4-bit quantization of attention maps and utilize the BitShift operator instead of multiplication during inference, which effectively reduces hardware resource requirement. Experimental results show that our fully quantized Vision Transformers achieve comparable performance with the full precision models. Altogether, we provide a higher baseline for future works, hoping that FQ-ViT’s strong performance

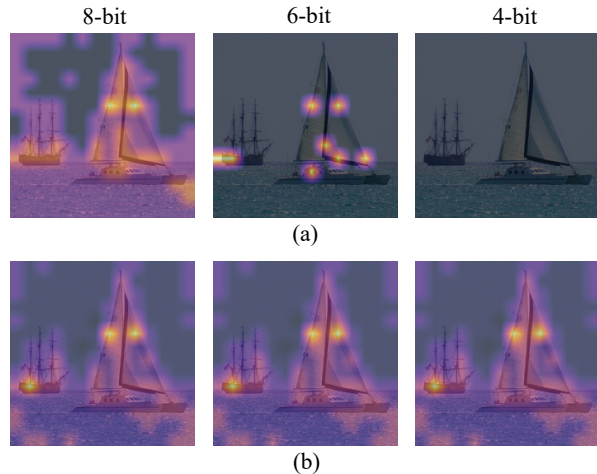


Figure 6: Attention map visualization. (a) shows the results of uniform quantization and (b) shows the results of Log2 quantization.

Model	FP	Int8	Int4		LIS
		Uni	Uni	Log2	
ViT-B	84.54	83.46	9.53	83.23	82.91
ViT-L	85.81	85.37	58.74	85.40	85.18
DeiT-T	72.21	71.74	8.69	71.46	71.05
DeiT-S	79.85	79.42	10.98	79.19	78.63
DeiT-B	81.84	81.48	23.07	81.41	81.06
Swin-T	81.35	80.70	77.86	80.45	80.17
Swin-S	83.22	82.94	81.82	82.73	82.63
Swin-B	83.59	83.26	81.28	83.14	82.80

Table 4: Comparison between 8-bit and 4-bit with uniform, Log2 quantization. The last column shows the integer-only inference won’t affect much on performance.

will encourage research into even lower bit-width quantization of Vision Transformers, which will boost their real-world adoptions.

References

- [1] Jimmy Lei Ba, Jamie Ryan Kiros, and Geoffrey E Hinton. Layer normalization. *arXiv preprint arXiv:1607.06450*, 2016. 3
- [2] Jingyong Cai, Masashi Takemoto, and Hironori Nakajo. A deep look into logarithmic quantization of model parameters in neural networks. In *Proceedings of the 10th International Conference on Advances in Information Technology*, pages 1–8, 2018. 2
- [3] Zhaowei Cai and Nuno Vasconcelos. Cascade r-cnn: Delving into high quality object detection. In *Proceedings of the IEEE Conference on Computer Vision and Pattern Recognition*, pages 6154–6162, 2018. 6
- [4] Nicolas Carion, Francisco Massa, Gabriel Synnaeve, Nicolas Usunier, Alexander Kirillov, and Sergey Zagoruyko. End-to-end object detection with transformers. In *European Conference on Computer Vision*, pages 213–229. Springer, 2020. 1, 2

- [5] Hanting Chen, Yunhe Wang, Tianyu Guo, Chang Xu, Yiping Deng, Zhenhua Liu, Siwei Ma, Chunjing Xu, Chao Xu, and Wen Gao. Pre-trained image processing transformer. In *Proceedings of the IEEE/CVF Conference on Computer Vision and Pattern Recognition*, pages 12299–12310, 2021. [2](#)
- [6] Cheng Chi, Fangyun Wei, and Han Hu. Relationnet++: Bridging visual representations for object detection via transformer decoder. In Hugo Larochelle, Marc’Aurelio Ranzato, Raia Hadsell, Maria-Florina Balcan, and Hsuan-Tien Lin, editors, *Advances in Neural Information Processing Systems 33: Annual Conference on Neural Information Processing Systems 2020, NeurIPS 2020, December 6-12, 2020, virtual*, 2020. [2](#)
- [7] Jungwook Choi, Zhuo Wang, Swagath Venkataramani, Pierce I-Jen Chuang, Vijayalakshmi Srinivasan, and Kailash Gopalakrishnan. Pact: Parameterized clipping activation for quantized neural networks. *arXiv preprint arXiv:1805.06085*, 2018. [2](#)
- [8] Yoni Choukroun, Eli Kravchik, Fan Yang, and Pavel Kisilev. Low-bit quantization of neural networks for efficient inference. In *2019 IEEE/CVF International Conference on Computer Vision Workshops, ICCV Workshops 2019, Seoul, Korea (South), October 27-28, 2019*, pages 3009–3018. IEEE, 2019. [2](#), [5](#), [6](#)
- [9] Alexey Dosovitskiy, Lucas Beyer, Alexander Kolesnikov, Dirk Weissenborn, Xiaohua Zhai, Thomas Unterthiner, Mostafa Dehghani, Matthias Minderer, Georg Heigold, Sylvain Gelly, Jakob Uszkoreit, and Neil Houlsby. An image is worth 16x16 words: Transformers for image recognition at scale. In *International Conference on Learning Representations*, 2021. [1](#), [2](#), [4](#), [6](#)
- [10] Steven K. Esser, Jeffrey L. McKinstry, Deepika Bablani, Rathinakumar Appuswamy, and Dharmendra S. Modha. Learned step size quantization. In *International Conference on Learning Representations*, 2020. [1](#), [2](#)
- [11] Ruihao Gong, Xianglong Liu, Shenghu Jiang, Tianxiang Li, Peng Hu, Jiazhen Lin, Fengwei Yu, and Junjie Yan. Differentiable soft quantization: Bridging full-precision and low-bit neural networks. In *2019 IEEE/CVF International Conference on Computer Vision, ICCV 2019, Seoul, Korea (South), October 27 - November 2, 2019*, pages 4851–4860. IEEE, 2019. [2](#)
- [12] Ben Graham, Alaeldin El-Nouby, Hugo Touvron, Pierre Stock, Armand Joulin, Hervé Jégou, and Matthijs Douze. Levit: a vision transformer in convnet’s clothing for faster inference. *arXiv preprint arXiv:2104.01136*, 2021. [1](#), [2](#)
- [13] Yiwen Guo, Anbang Yao, and Yurong Chen. Dynamic network surgery for efficient dnns. In Daniel D. Lee, Masashi Sugiyama, Ulrike von Luxburg, Isabelle Guyon, and Roman Garnett, editors, *Advances in Neural Information Processing Systems 29: Annual Conference on Neural Information Processing Systems 2016, December 5-10, 2016, Barcelona, Spain*, pages 1379–1387, 2016. [1](#)
- [14] Kai Han, An Xiao, Enhua Wu, Jianyuan Guo, Chunjing Xu, and Yunhe Wang. Transformer in transformer. *arXiv preprint arXiv:2103.00112*, 2021. [2](#)
- [15] Song Han, Huizi Mao, and William J Dally. Deep compression: Compressing deep neural networks with pruning, trained quantization and Huffman coding. In *International Conference on Learning Representations*, 2016. [1](#)
- [16] Ali Hassani, Steven Walton, Nikhil Shah, Abulikemu Abuduweili, Jiachen Li, and Humphrey Shi. Escaping the big data paradigm with compact transformers. *arXiv preprint arXiv:2104.05704*, 2021. [2](#)
- [17] Kaiming He, Georgia Gkioxari, Piotr Dollár, and Ross B. Girshick. Mask R-CNN. In *IEEE International Conference on Computer Vision, ICCV 2017, Venice, Italy, October 22-29, 2017*, pages 2980–2988. IEEE Computer Society, 2017. [6](#)
- [18] Kaiming He, Xiangyu Zhang, Shaoqing Ren, and Jian Sun. Deep residual learning for image recognition. In *Proceedings of the IEEE Conference on Computer Vision and Pattern Recognition*, pages 770–778, 2016. [3](#)
- [19] Geoffrey Hinton, Oriol Vinyals, and Jeff Dean. Distilling the knowledge in a neural network. *arXiv preprint arXiv:1503.02531*, 2015. [1](#)
- [20] Andrew G Howard, Menglong Zhu, Bo Chen, Dmitry Kalenichenko, Weijun Wang, Tobias Weyand, Marco Andreetto, and Hartwig Adam. Mobilenets: Efficient convolutional neural networks for mobile vision applications. *arXiv preprint arXiv:1704.04861*, 2017. [1](#)
- [21] Itay Hubara, Yury Nahshan, Yair Hanani, Ron Banner, and Daniel Soudry. Accurate post training quantization with small calibration sets. In Marina Meila and Tong Zhang, editors, *Proceedings of the 38th International Conference on Machine Learning*, volume 139 of *Proceedings of Machine Learning Research*, pages 4466–4475. PMLR, 18–24 Jul 2021. [2](#)
- [22] Sergey Ioffe and Christian Szegedy. Batch normalization: Accelerating deep network training by reducing internal covariate shift. In Francis R. Bach and David M. Blei, editors, *Proceedings of the 32nd International Conference on Machine Learning, ICML 2015, Lille, France, 6-11 July 2015*, volume 37 of *JMLR Workshop and Conference Proceedings*, pages 448–456. JMLR.org, 2015. [3](#)
- [23] Benoit Jacob, Skirmantas Kligys, Bo Chen, Menglong Zhu, Matthew Tang, Andrew Howard, Hartwig Adam, and Dmitry Kalenichenko. Quantization and training of neural networks for efficient integer-arithmetic-only inference. In *Proceedings of the IEEE Conference on Computer Vision and Pattern Recognition*, pages 2704–2713, 2018. [2](#), [5](#), [6](#)
- [24] Zihang Jiang, Qibin Hou, Li Yuan, Daquan Zhou, Yujun Shi, Xiaojie Jin, Anran Wang, and Jiashi Feng. All tokens matter: Token labeling for training better vision transformers. *arXiv preprint arXiv:2104.10858*, 2021. [2](#)
- [25] Sehoon Kim, Amir Gholami, Zhewei Yao, Michael W. Mahoney, and Kurt Keutzer. I-BERT: integer-only BERT quantization. In Marina Meila and Tong Zhang, editors, *Proceedings of the 38th International Conference on Machine Learning, ICML 2021, 18-24 July 2021, Virtual Event*, volume 139 of *Proceedings of Machine Learning Research*, pages 5506–5518. PMLR, 2021. [1](#), [5](#), [11](#)
- [26] Alex Krizhevsky, Ilya Sutskever, and Geoffrey E. Hinton. Imagenet classification with deep convolutional neural networks. In Peter L. Bartlett, Fernando C. N. Pereira, Christopher J. C. Burges, Léon Bottou, and Kilian Q. Weinberger, editors, *Advances in Neural Information Processing Systems 25: 26th Annual Conference on Neural Information Processing Systems 2012. Proceedings of a meeting held December 3-6, 2012, Lake Tahoe, Nevada, United States*, pages 1106–1114, 2012. [5](#), [6](#)
- [27] Rundong Li, Yan Wang, Feng Liang, Hongwei Qin, Junjie Yan, and Rui Fan. Fully quantized network for object detection. In *Proceedings of the IEEE/CVF Conference on Computer Vision and Pattern Recognition*, pages 2810–2819, 2019. [5](#), [6](#)
- [28] Yuhang Li, Ruihao Gong, Xu Tan, Yang Yang, Peng Hu, Qi Zhang, Fengwei Yu, Wei Wang, and Shi Gu. Brecq: Pushing

- the limit of post-training quantization by block reconstruction. In *International Conference on Learning Representations*, 2021. 2
- [29] Xiaocong Lian, Zhenyu Liu, Zhourui Song, Jiwei Dai, Wei Zhou, and Xiangyang Ji. High-performance fpga-based cnn accelerator with block-floating-point arithmetic. *IEEE Transactions on Very Large Scale Integration (VLSI) Systems*, 27(8):1874–1885, 2019. 4
- [30] Tsung-Yi Lin, Michael Maire, Serge Belongie, James Hays, Pietro Perona, Deva Ramanan, Piotr Dollár, and C Lawrence Zitnick. Microsoft coco: Common objects in context. In *European Conference on Computer Vision*, pages 740–755. Springer, 2014. 5, 6
- [31] Ze Liu, Yutong Lin, Yue Cao, Han Hu, Yixuan Wei, Zheng Zhang, Stephen Lin, and Baining Guo. Swin transformer: Hierarchical vision transformer using shifted windows. *arXiv preprint arXiv:2103.14030*, 2021. 1, 2, 6
- [32] Zhenhua Liu, Yunhe Wang, Kai Han, Wei Zhang, Siwei Ma, and Wen Gao. Post-training quantization for vision transformer. In *Thirty-Fifth Conference on Neural Information Processing Systems*, 2021. 1, 2, 4, 5
- [33] Markus Nagel, Rana Ali Amjad, Mart van Baalen, Christos Louizos, and Tijmen Blankevoort. Up or down? adaptive rounding for post-training quantization. In *Proceedings of the 37th International Conference on Machine Learning, ICML 2020, 13-18 July 2020, Virtual Event*, volume 119 of *Proceedings of Machine Learning Research*, pages 7197–7206. PMLR, 2020. 1, 2
- [34] Yongming Rao, Wenliang Zhao, Benlin Liu, Jiwei Lu, Jie Zhou, and Cho-Jui Hsieh. Dynamicvit: Efficient vision transformers with dynamic token sparsification. *arXiv preprint arXiv:2106.02034*, 2021. 2, 4
- [35] Victor Sanh, Lysandre Debut, Julien Chaumond, and Thomas Wolf. Distilbert, a distilled version of bert: smaller, faster, cheaper and lighter. *arXiv preprint arXiv:1910.01108*, 2019. 1
- [36] Sheng Shen, Zhen Dong, Jiayu Ye, Linjian Ma, Zhewei Yao, Amir Gholami, Michael W Mahoney, and Kurt Keutzer. Q-bert: Hessian based ultra low precision quantization of bert. In *Proceedings of the AAAI Conference on Artificial Intelligence*, volume 34, pages 8815–8821, 2020. 1
- [37] Robin Strudel, Ricardo Garcia, Ivan Laptev, and Cordelia Schmid. Segmenter: Transformer for semantic segmentation. *arXiv preprint arXiv:2105.05633*, 2021. 2
- [38] Mingxing Tan and Quoc V. Le. Efficientnet: Rethinking model scaling for convolutional neural networks. In Kamalika Chaudhuri and Ruslan Salakhutdinov, editors, *Proceedings of the 36th International Conference on Machine Learning, ICML 2019, 9-15 June 2019, Long Beach, California, USA*, volume 97 of *Proceedings of Machine Learning Research*, pages 6105–6114. PMLR, 2019. 1, 4
- [39] Hugo Touvron, Matthieu Cord, Matthijs Douze, Francisco Massa, Alexandre Sablayrolles, and Hervé Jégou. Training data-efficient image transformers & distillation through attention. In Marina Meila and Tong Zhang, editors, *Proceedings of the 38th International Conference on Machine Learning, ICML 2021, 18-24 July 2021, Virtual Event*, volume 139 of *Proceedings of Machine Learning Research*, pages 10347–10357. PMLR, 2021. 1, 2, 6
- [40] Ashish Vaswani, Noam Shazeer, Niki Parmar, Jakob Uszkoreit, Llion Jones, Aidan N. Gomez, Lukasz Kaiser, and Illia Polosukhin. Attention is all you need. In Isabelle Guyon, Ulrike von Luxburg, Samy Bengio, Hanna M. Wallach, Rob Fergus, S. V. N. Vishwanathan, and Roman Garnett, editors, *Advances in Neural Information Processing Systems 30: Annual Conference on Neural Information Processing Systems 2017, December 4-9, 2017, Long Beach, CA, USA*, pages 5998–6008, 2017. 2
- [41] Wenhai Wang, Enze Xie, Xiang Li, Deng-Ping Fan, Kaitao Song, Ding Liang, Tong Lu, Ping Luo, and Ling Shao. Pyramid vision transformer: A versatile backbone for dense prediction without convolutions. *arXiv preprint arXiv:2102.12122*, 2021. 2
- [42] Zhendong Wang, Xiaodong Cun, Jianmin Bao, and Jianzhuang Liu. Uformer: A general u-shaped transformer for image restoration. *arXiv preprint arXiv:2106.03106*, 2021. 2
- [43] Haiping Wu, Bin Xiao, Noel Codella, Mengchen Liu, Xiyang Dai, Lu Yuan, and Lei Zhang. Cvt: Introducing convolutions to vision transformers. *arXiv preprint arXiv:2103.15808*, 2021. 2
- [44] Yifan Xu, Zhijie Zhang, Mengdan Zhang, Kekai Sheng, Ke Li, Weiming Dong, Liqing Zhang, Changsheng Xu, and Xing Sun. Evo-vit: Slow-fast token evolution for dynamic vision transformer. *arXiv preprint arXiv:2108.01390*, 2021. 2
- [45] Wei Zhang, Lu Hou, Yichun Yin, Lifeng Shang, Xiao Chen, Xin Jiang, and Qun Liu. Ternarybert: Distillation-aware ultra-low bit BERT. In Bonnie Webber, Trevor Cohn, Yulan He, and Yang Liu, editors, *Proceedings of the 2020 Conference on Empirical Methods in Natural Language Processing, EMNLP 2020, Online, November 16-20, 2020*, pages 509–521. Association for Computational Linguistics, 2020. 5
- [46] Sixiao Zheng, Jiachen Lu, Hengshuang Zhao, Xiatian Zhu, Zekun Luo, Yabiao Wang, Yanwei Fu, Jianfeng Feng, Tao Xiang, Philip HS Torr, et al. Rethinking semantic segmentation from a sequence-to-sequence perspective with transformers. In *Proceedings of the IEEE/CVF Conference on Computer Vision and Pattern Recognition*, pages 6881–6890, 2021. 1, 2
- [47] Shuchang Zhou, Yuxin Wu, Zekun Ni, Xinyu Zhou, He Wen, and Yuheng Zou. Dorefa-net: Training low bitwidth convolutional neural networks with low bitwidth gradients. *arXiv preprint arXiv:1606.06160*, 2016. 1, 2
- [48] Xizhou Zhu, Weijie Su, Lewei Lu, Bin Li, Xiaogang Wang, and Jifeng Dai. Deformable detr: Deformable transformers for end-to-end object detection. In *International Conference on Learning Representations*, 2021. 2

A Appendix

A.1 Quantized Inference

Quantized Inference of LayerNorm LayerNorm has been widely used in neural networks to accelerate the convergence during the training process, which can be formulated as:

$$y = \frac{X - \mu_X}{\sqrt{\sigma_X^2 + \epsilon}} \cdot \gamma + \beta \quad (20)$$

$$= \frac{\gamma}{\sqrt{\sigma_X^2 + \epsilon}} X + \frac{\beta\sqrt{\sigma_X^2 + \epsilon} - \gamma\mu_X}{\sqrt{\sigma_X^2 + \epsilon}}, \quad (21)$$

where γ, β are the learned parameters and μ_X, σ_X are the statistics which need to be calculated based on the input of LayerNorm.

In this paper, proposed Powers-of-Two Scale is used for LayerNorm input $X \in \mathbb{R}^{B \times L \times C}$ and its quantized value X_Q can be written as:

$$X_Q = Q(X|b) = \text{clip}(\lfloor \frac{X}{2^P S} \rfloor + Z, 0, 2^b - 1), \quad (22)$$

where $S, Z \in \mathbb{R}$ are quantization parameters and $P \in \mathbb{R}^C$ is Powers-of-Two Scale factor.

Following the LayerNorm's definition, we should calculate the statistics of input X . As described in this paper, the whole process can be divided into two phases. In the first phase, we shift the quantized activation X_Q with factors P :

$$\hat{X}_Q = (X_Q - Z) \ll P. \quad (23)$$

Then, in the second phase, we need to calculate the statistics based on the shifted activation \hat{X}_Q . Firstly, we gauge the mean of X and X^2 as follows:

$$\mu_X \approx \frac{1}{C} \sum_{i=1}^C (\hat{X}_{Qi} \cdot S) = \frac{S}{C} \sum_{i=1}^C (\hat{X}_{Qi}) \rightarrow \frac{S}{C} M_1, \quad (24)$$

$$\mu_{X^2} \approx \frac{1}{C} \sum_{i=1}^C (\hat{X}_{Qi} \cdot S)^2 = \frac{S^2}{C} \sum_{i=1}^C (\hat{X}_{Qi})^2 \rightarrow \frac{S^2}{C} M_2, \quad (25)$$

where C is the number of channels in X . Secondly, we utilize μ_X and μ_{X^2} to calculate σ_X^2 :

$$\sigma_X^2 = \mu_{X^2} - \mu_X^2 \approx \frac{S^2}{C^2} (CM_2 - M_1^2), \quad (26)$$

and approximate $\sqrt{\sigma_X^2 + \epsilon}$ as:

$$\sqrt{\sigma_X^2 + \epsilon} \approx \frac{S}{C} \sqrt{CM_2 - M_1^2}. \quad (27)$$

Thus, we obtain the statistics of input X based on integer-only calculations.

After the calculations of statistics, we need to do the integrated inference of LayerNorm. Equation 20 can be written as follows by quantizing the input X and output y :

$$y_Q = \lfloor \frac{S_{in}\gamma}{S_{out}\sqrt{\sigma_X^2 + \epsilon}} \hat{X}_Q + \frac{\beta\sqrt{\sigma_X^2 + \epsilon} - \gamma\mu_X}{S_{out}\sqrt{\sigma_X^2 + \epsilon}} \rfloor + Z_{out}, \quad (28)$$

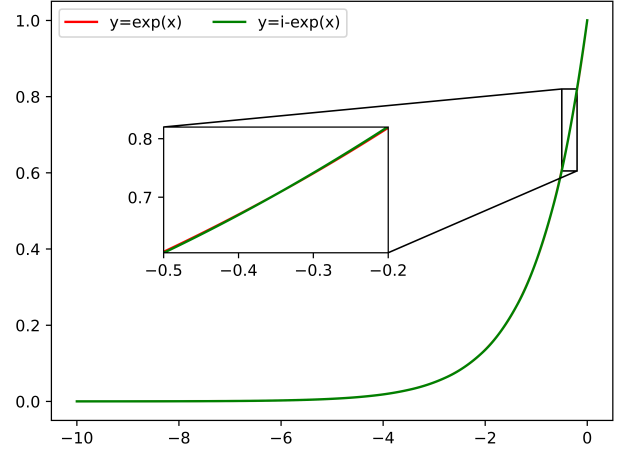


Figure 7: Comparison between exponential function (exp) and integer-only exponential function (i-exp)

where $S_{in} \in \mathbb{R}^1$ is the scale of input X , and $S_{out}, Z_{out} \in \mathbb{R}^1$ are the scale of output y .

In order to simplify the equation, we fuse each term as follows:

$$A = \frac{S_{in}\gamma}{S_{out}\sqrt{\sigma_X^2 + \epsilon}}, \quad (29)$$

$$B = \frac{\beta\sqrt{\sigma_X^2 + \epsilon} - \gamma\mu_X}{S_{out}\sqrt{\sigma_X^2 + \epsilon}}. \quad (30)$$

To obtain the integer-only inference, we approximate A as:

$$N_1 = b - \lfloor \log_2 A \rfloor, N_2 = \lfloor A2^{N_1} \rfloor, \quad (31)$$

$$A \approx \frac{N_2}{2^{N_1}}. \quad (32)$$

Finally, the quantized inference for LayerNorm can be formulated as:

$$y_Q = \lfloor A\hat{X}_Q + B \rfloor + Z_{out} \quad (33)$$

$$= \lfloor \frac{N_2\hat{X}_Q + \lfloor B \cdot 2^{N_1} \rfloor}{2^{N_1}} \rfloor + Z_{out}. \quad (34)$$

Quantized Inference of Softmax Softmax is generally used in the Vision Transformers and it can be formulated as:

$$\text{Softmax}(X)_i = \frac{\exp(X_i)}{\sum_{j=1}^J \exp(X_j)}. \quad (35)$$

In practice, we subtract the maximum value of the input to avoid overflowing:

$$\tilde{X}_i = X_i - \max(X), \quad (36)$$

and thus the Softmax can be written as:

$$\text{Softmax}(X)_i = \frac{\exp(\tilde{X}_i)}{\sum_{j=1}^J \exp(\tilde{X}_j)}. \quad (37)$$

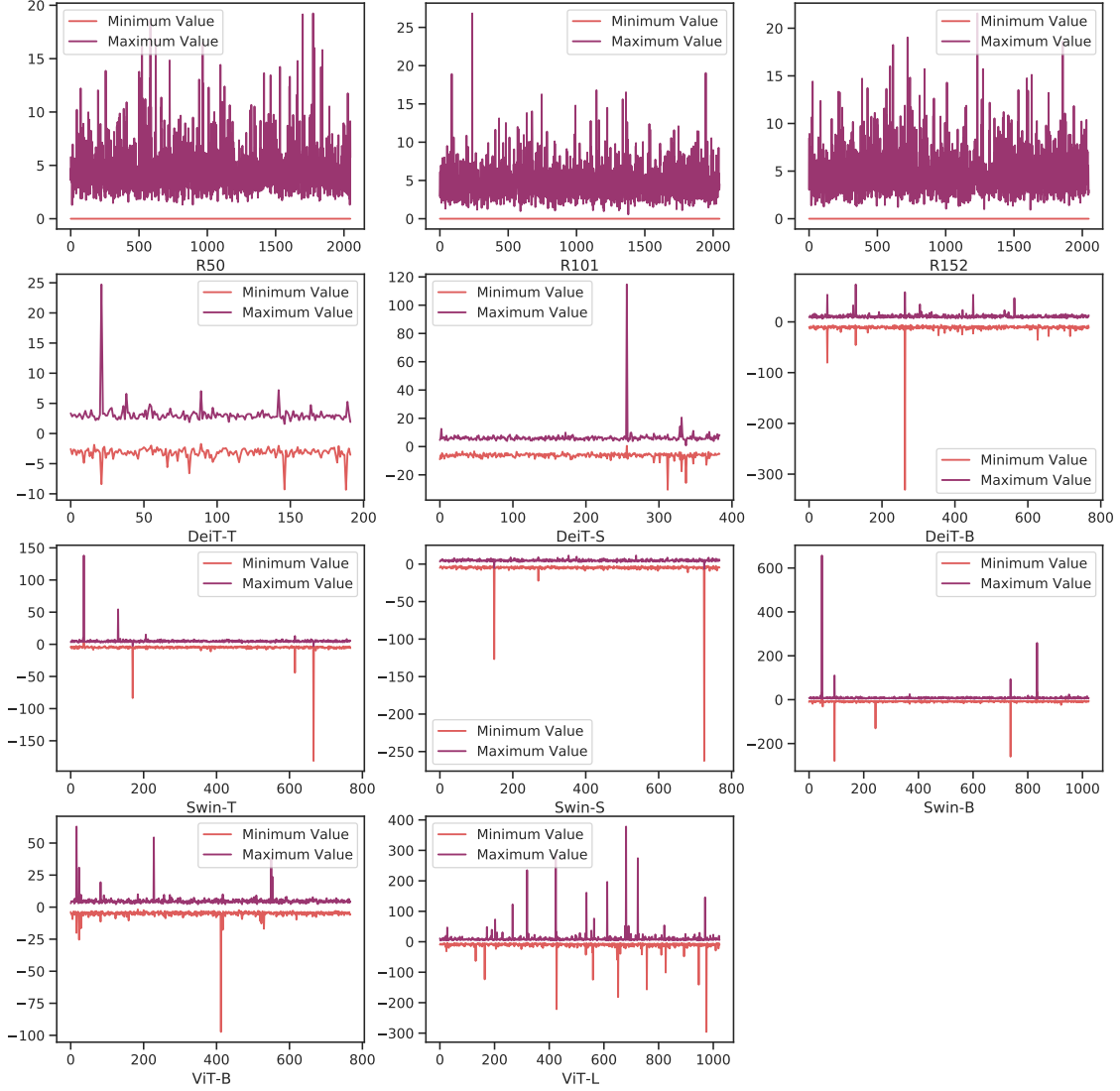


Figure 8: Channel-wise minimum and maximum values of Vision Transformers and ResNets.

Now, all inputs, \tilde{X} , become non-positive. We decompose it as $(-\ln 2)z + p$, where z is a non-negative integer and the p is a real number in $(-\ln 2, 0]$. Then, the exponential of \tilde{X} can be written as:

$$\exp(\tilde{X}) = 2^{-z} \exp(p) = \exp(p) \gg z, \quad (38)$$

where \gg is the right shifting.

[25] uses a second-order polynomial to approximate the exponential function in the interval of $p \in (-\ln 2, 0]$:

$$L(p) = 0.3585(p + 1.353)^2 + 0.344 \approx \exp(p), \quad (39)$$

$$\exp(\tilde{x}) \approx \text{i-exp}(\tilde{x}) := L(p) \gg z, \quad (40)$$

where $z = \lfloor -\tilde{X} / \ln 2 \rfloor$ and $p = \tilde{X} + z \ln 2$.

Figure 7 plots the result of i-exp, which is nearly identical to the exponential function. The largest gap between these two functions is only 1.9×10^{-3} , which is relatively

negligible comparing to 8-bit quantization error of $1/255 = 3.9 \times 10^{-3}$.

Based on i-exp (Algorithm 1), we propose Log-Int-Softmax (LIS) as Algorithm 2 shows. Firstly, the maximum value of inputs is subtracted to ensure all the inputs are non-positive, and the results are sent to the i-exp. After that, we replace the original Softmax by its reciprocal to ensure the results of integer division to be larger than 1. Last but not least, we perform a Log2 quantization on the output of reverse Softmax as:

$$\text{LIS}(S \cdot X_Q) = N - \text{clip}(\log_2 \lfloor \frac{\sum \text{i-exp}(X_Q)}{\text{i-exp}(X_Q)} \rfloor, 0, 2^b - 1) \quad (41)$$

$$= N - \text{Attn}_Q, \quad (42)$$

with $N = 2^b - 1$. X_Q, S are the quantized input and scale.

Algorithm 1: Integer-only Exponential Function

Input: q, S : quantized input and scale**Output:** q_{out}, S_{out} : quantized output and scale**function** I-EXP(q, S) $q_{ln2} \leftarrow \lfloor -\ln 2/S \rfloor$ $q \leftarrow \max(q, n \cdot q_{ln2})$ $z \leftarrow \lfloor q/q_{ln2} \rfloor$ $q_p \leftarrow q - z \cdot q_{ln2}$ $q_b, q_c \leftarrow \lfloor b/S \rfloor, \lfloor c/a.S^2 \rfloor$ $S_L \leftarrow \lfloor a.S^2 \rfloor$ $q_L = (q + q_b)^2 + q_c$ $q_{out}, S_{out} \leftarrow q_L \ll n - z, S_L/2^n$ **return** q_{out}, S_{out} **end function**

Algorithm 2: Log-Int-Softmax

Input: q, S : quantized input and input scale**Output:** q_{out}, S_{out} : quantized output and output scale**function** I-LOG2(q) $M \leftarrow \text{Find_First_One}(q)$ $\chi \leftarrow (M - 1)^{th} \text{ Bit of } q$ $q_{out} \leftarrow M + \chi$ **return** q_{out} **end function****function** LOG-INT-SOFTMAX(q, S) $\tilde{q} \leftarrow q - \max(q)$ $q_{exp}, S_{exp} \leftarrow \text{I-Exp}(\tilde{q}, S)$ $q_{rev} \leftarrow \lfloor \text{sum}(q_{exp})/q_{exp} \rfloor$ $q_{out}, S_{out} \leftarrow N - \text{I-Log2}(q_{rev}), 1/2^N$ **return** q_{out}, S_{out} **end function**

The Log2 function can be calculated with integer arithmetic as showed in Algorithm 2. To obtain the Log2 of the integer, we introduce the Find_First_One function which returns the index of the most significant one bit of the input. The whole process can be done in integer domain. For example, if the input of I-Log2 is 0000 1101 1010 1100₂, the M, χ will be calculated as 11, 1 and the rounding result will be 12.

The following step of Softmax is the matrix multiplication between attention map Attn and values V . Considering V_Q is the quantized value of V and its scale and zero point are $S_V, Z_V \in \mathbb{R}$, the matrix multiplication can be written as:

$$\text{Attn} \cdot V = \frac{2^{N-\text{AttnQ}}}{2^N} \cdot (V_Q - Z_V)S_V \quad (43)$$

$$= \frac{S_V}{2^N} \cdot (V_Q - Z_V) \ll (N - \text{AttnQ}). \quad (44)$$

As we can see, the multiplication is converted to BitShift operator with an output scale $\frac{S_V}{2^N}$, where N equals $2^4 - 1 = 15$ in 4-bit quantization.

Based on the above processes, we realize fully fixed-point inference for Softmax and accelerate the calculation of attention map and values by using BitShift.

A.2 Inter-channel Variation for Vision Transformers and ResNets

In Figure 8, we present the channel-wise minimum and maximum values of Vision Transformers and ResNets. For comparison, we choose the input of the last LayerNorm layer for Vision Transformers and the output of the fourth stage for ResNets to show. It is observed that a serious inter-channel variation are found in Vision Transformers.